

Brief Reports

Brief Reports are short papers which report on completed research or are addenda to papers previously published in the Physical Review. A Brief Report may be no longer than 3½ printed pages and must be accompanied by an abstract.

 $^{13}\text{C}(\pi^+, \pi^-)^{13}\text{O}$ near the Δ_{33} resonance

Peter A. Seidl, Mark D. Brown, Rex R. Kiziah, and C. Fred Moore
University of Texas at Austin, Austin, Texas 78712

Helmut Baer and C. L. Morris
Los Alamos National Laboratory, Los Alamos, New Mexico 87545

G. R. Burlison, W. B. Cottingham and Steven J. Greene*
New Mexico State University, Las Cruces, New Mexico 88003

L. C. Bland† and R. Gilman
University of Pennsylvania, Philadelphia, Pennsylvania 19104

H. T. Fortune‡
Los Alamos National Laboratory, Los Alamos, New Mexico 87545
and University of Pennsylvania, Philadelphia, Pennsylvania 19104
 (Received 9 April 1984)

We present differential cross sections for $^{13}\text{C}(\pi^+, \pi^-)^{13}\text{O}(\text{g.s.})$ and $^{13}\text{C}(\pi^+, \pi^-)^{13}\text{O}(4.21 \text{ MeV})$ near the Δ_{33} resonance. The former exhibits a slowly varying angular distribution between 0° and 50° , but the excited state angular distribution shows diffractive features observed formerly only in $J^\pi=0^+$ to 0^+ non-analog double-charge-exchange reactions.

Most angular-distribution and excitation-function data for (π^+, π^-) near the Δ_{33} resonance are of the type $J_i^\pi = J_f^\pi = 0^+$. Nonanalog double-double-exchange (DCX) data on odd A nuclei are limited. The angular distributions and excitation functions for (π^+, π^-) DCX on $T=0$ target nuclei exhibit a common set of features.¹ The angular distributions are forward peaked and possess minima consistent with a (strongly absorptive) diffractive process. The excitation functions peak at $T_\pi \approx 160$ MeV and have widths of approximately 70 MeV, and the target mass dependence is roughly $A^{-4/3}$ for $12 \leq A \leq 56$. No measurements for $A > 56$ have been reported. These characteristics are contrasted with the irregular mass and energy dependence, and nondiffractive angular distributions for DCX on $T \geq 1$ nuclei leading to the double isobaric analog state (DIAS).^{2,3} Some of the analog data have been explained by phenomenological second order calculations,⁴ second order calculations including core excitation effects,⁵ or the interference of an analog and nonanalog amplitude.⁶ However, the first two approaches do not simultaneously address nonanalog DCX data.

It became of interest to measure DCX cross sections on ^{13}C , an odd- A target for which data on the neighboring isotopes ^{12}C and ^{14}C would also be available. The present experiment on ^{13}C was performed at the Energetic Pion Channel and Spectrometer⁷ (EPICS) at the Clinton P. Anderson Meson Physics Facility. A dipole magnet was installed after the target, with \vec{B} perpendicular to the scattering plane.⁸ This DCX modification to EPICS separates positive from negative pions in the scattered beam by 20° , facilitating measurements of forward angle cross sections. The

geometry of the targets with respect to the dispersed incident beam is described in Refs. 2 and 8, and the ^{13}C data reported here were collected simultaneously with the ^{14}C , $^{26}\text{Mg}(\pi^+, \pi^-)^{14}\text{O}$, ^{26}Si measurements reported in Ref. 2.

Two ^{13}C targets of 90% isotopic purity were used. The thick target (1489 mg/cm²) was used for all of the new measurements reported. The thin target (706 mg/cm²) was included for the measurements at $T_\pi=292$ MeV and was analyzed separately from the thick target data. The cross sections at 292 MeV are weighted averages of yields from the thick and thin targets. Normalization of the data was obtained by measuring $^1\text{H}(\pi^+, \pi^+)$ yields at 50° , and comparing them to cross sections calculated from the phase shift analysis of Carter, Bugg, and Carter.⁹ The error bars plotted in Figs. 2 and 3 include only the statistical uncertainties of the DCX and $^1\text{H}(\pi^+, \pi^+)$ peak areas. The overall normalization is accurate to $\pm 10\%$.

Resolutions of missing mass spectra for the thick and thin targets are 0.9 and 0.5 MeV full-width at half maximum (FWHM), respectively. Two spectra, containing all data collected with the thick target at $T_\pi=164$ and 292 MeV, are shown in Fig. 1. The onset of particle instability— $^{12}\text{N}+p$ and $^{11}\text{C}+2p$ above $E_x=1.53$ and 2.12 MeV—is evident in the spectra. Little else is known about the nuclear structure of ^{13}O . The $T_\pi=164$ MeV spectrum shows evidence for an excited state at $E_x=2.75 \pm 0.04$ MeV, in agreement with the ^{13}O spectrum measured with the $^{12}\text{C}(p, \pi^-)^{13}\text{O}$ reaction,¹⁰ where a state has been observed at 2.82 ± 0.24 MeV. Our 164 MeV spectrum shows an enhancement at 6.02 ± 0.08 MeV, with a FWHM of 1.2 MeV and may be due to the ex-

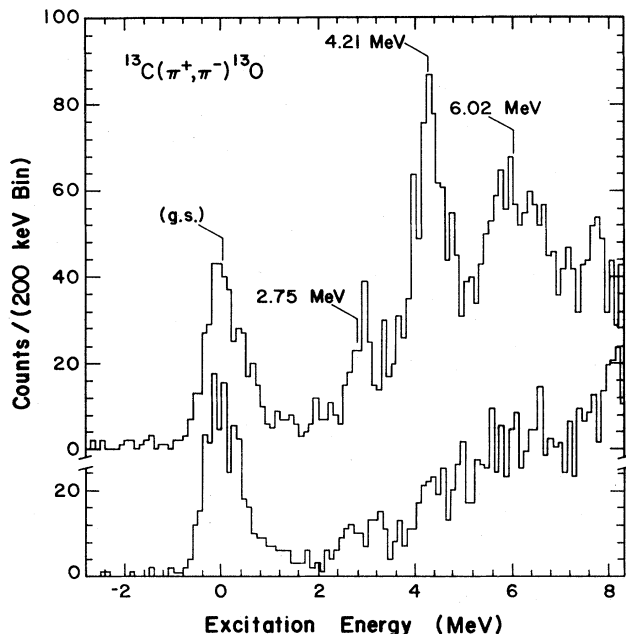


FIG. 1. Missing mass spectra for $^{13}\text{C}(\pi^+, \pi^-)^{13}\text{O}$ at $T_\pi = 164$ (top) and 292 MeV (bottom), measured with the target of areal density 1489 mg/cm². The spectra are the raw number of counts summed over all angles for which data were taken and are not corrected for spectrometer acceptance as a function of outgoing pion momentum.

citation of more than one state. The state at 4.21 MeV is the only one to have a large enough cross section to facilitate the extraction of an angular distribution—the existence of the continuum background prevents a reliable determination of peak areas for the more weakly excited states. There is no evidence for any of these excited states in the 292 MeV spectrum.

The excitation functions for $^{13}\text{C}(\pi^+, \pi^-)^{13}\text{O}$ (0.0 MeV, 4.21 MeV) are shown in Fig. 2. The ^{13}O (g.s.) excitation function decreases by a factor of 2.5 between 119 and 180 MeV and the new datum at 180 MeV agrees well with the previous measurement of Ref. 11. The cross sections at $T_\pi = 164$ and 292 MeV are roughly equal, in contrast to the excitation function for the only other nonanalog DCX measurement on a $T = \frac{1}{2}$ target, $^{11,12} \text{Be}(\pi^+, \pi^-)^9\text{C}$ (g.s.), which monotonically decreases by a factor of 8 between $T_\pi = 140$ and 295 MeV. In a simple shell model, the $^9\text{Be}(\pi^+, \pi^-)^9\text{C}$ (g.s.) reaction can proceed via

$$\nu(p_{3/2})^3\pi(p_{3/2})^2 \rightarrow \nu(p_{3/2})^1\pi(p_{3/2})^4,$$

while the $^{13}\text{C}(\pi^+, \pi^-)^{13}\text{O}$ (g.s.) reaction must necessarily change the orbits of nucleons. In the latter reaction, the relatively large cross section at $T_\pi = 292$ MeV is a feature common to analog DCX excitation functions, while the $^9\text{Be}(\pi^+, \pi^-)^9\text{C}$ (g.s.) excitation function resembles those for (ground state) to (ground state), $\Delta J = 0$, nonanalog DCX on $T = 0$ targets. These features of the data are indicative of interesting nuclear structure or momentum dependence effects.

The excitation function for the $E_x = 4.21$ MeV state gives only upper limits for the cross sections at 119 and 292 MeV and at 164 MeV exhibits cross sections about twice as large as that of the transition to the ground state. The energy

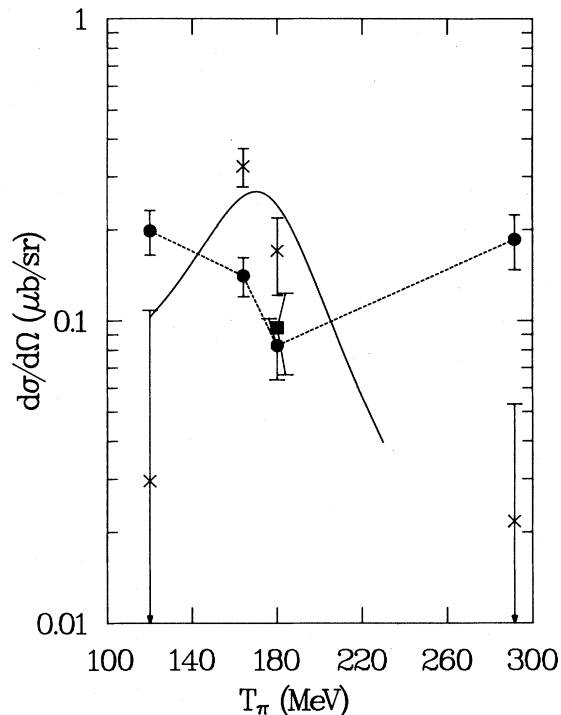


FIG. 2. Excitation function for $^{13}\text{C}(\pi^+, \pi^-)^{13}\text{O}$ (g.s.) for which the square is from Ref. 11 and the circles are from this work. The dashed line serves to guide the eye. The crosses are for $^{13}\text{C}(\pi^+, \pi^-)^{13}\text{O}$ (4.21 MeV). The solid line is a Breit-Wigner parametrization of the $^{12}\text{C}(\pi^+, \pi^-)^{12}\text{O}$ (g.s.) cross sections (Ref. 1), with a width and peak position of 60 and 178 MeV, respectively. The curve has been scaled down to the $^{13}\text{C}(\pi^+, \pi^-)^{13}\text{O}$ (4.21 MeV) excitation function.

dependence is similar to that measured for $^{12}\text{C}(\pi^+, \pi^-)^{12}\text{O}$ (g.s.) (Ref. 1) as shown in Fig. 2, and $^{14}\text{C}(\pi^+, \pi^-)^{14}\text{O}$ (5.9 MeV) (Ref. 2). Cross sections reported for the latter, a reaction where a low lying 0^+ state is strongly excited in addition to the DIAS, are due primarily to the 0_2^+ , 5.92 MeV state. Unfortunately, the resolution of the spectra in Ref. 2 prevented good separation of that state from the neighboring 3^- , 6.27 MeV state.

The 4.21 MeV state cross section at $T_\pi = 164$ MeV does not agree with the experimental $A^{-4/3}$ mass dependence of nonanalog DCX on self-conjugate targets: $\sigma(5^\circ)$ for the ^{13}O (4.21 MeV) is 0.50 ± 0.07 times that of the best fit $A^{-4/3}$ parametrization of the data in Ref. 1.

Figure 3 shows the angular distributions for $^{13}\text{C}(\pi^+, \pi^-)^{13}\text{O}$ (g.s.). At 164 MeV, the 0° and 50° cross section are roughly a factor of 2 lower than cross sections for $5^\circ \leq \theta \leq 40^\circ$. Other than this feature there is no strong angular dependence. At 292 MeV, $d\sigma/d\Omega$ is roughly constant for $0^\circ \leq \theta \leq 41^\circ$, and is decreased at 50° . We note that for the (ground state) to (ground state) transition, $J_i^\pi = \frac{1}{2}^-$ and $J_f^\pi = \frac{3}{2}^-$, which allows for the contribution of $\Delta J = 1$ and 2 processes in this transition. More than one multipole can also contribute to the $^9\text{Be}(\pi^+, \pi^-)^9\text{C}$ (g.s.) reaction,⁸ for which the angular distribution at $T_\pi = 162$ MeV is slowly varying for $5^\circ \leq \theta \leq 36^\circ$, and has a shallow minimum near 22° . Since the ground state angular distributions for both ^9Be and ^{13}C are not forward peaked, and the excitation functions differ, comparison of their A depen-

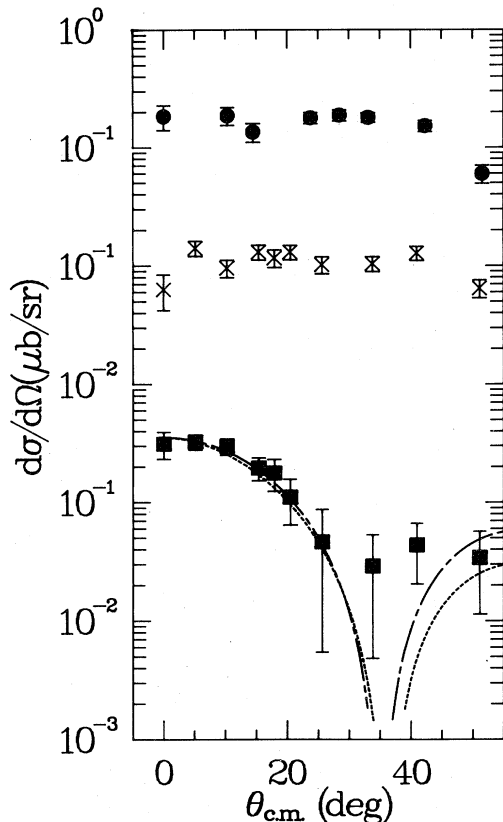


FIG. 3. Angular distributions for $^{13}\text{C}(\pi^+, \pi^-)^{13}\text{O}(\text{g.s.})$ are similar in shape and magnitude at both 164 (circles) and 292 MeV (crosses). The curves are $\sigma(\theta) = NJ_0^2(qR)e^{-qd}$, fit to the $^{13}\text{C}(\pi^+, \pi^-)^{13}\text{O}(4.21 \text{ MeV})$ data (squares). The long dashed curve is a best fit to the data: $R = 3.0 \pm 0.8$, $d = 0.1 \pm 1.1 \text{ fm}$, $\chi^2 = 0.77$, and $N = 0.39 \mu\text{b/sr}$. The short dashed curve has $R = 2.95 \text{ fm}$, $d = 0.61 \text{ fm}$, calculated from the two-tenths density point of a harmonic oscillator electron scattering parametrization (Ref. 14) of the charge distribution.

dence for 0^+ to 0^+ nonanalog DCX reactions is difficult. Comparisons should be made through angle-integrated cross sections, but existing nonanalog data are limited to $0^\circ \leq \theta \leq 50^\circ$.

The angular distribution (see Fig. 3) for the $E_x = 4.21 \text{ MeV}$ state is clearly forward peaked. The decrease in $d\sigma/d\Omega$ between 0° and 30° is similar to that observed for the $^{12}\text{C}(\pi^+, \pi^-)^{12}\text{O}(\text{g.s.})$ reaction¹ at 164 MeV. The data can be represented by the eikonal form¹³ $J_0^2(qR)e^{-qd}$, where q is the momentum transfer, R a suitable nuclear radius, and d the nuclear surface diffuseness. Figure 3 shows curves of damped Bessel functions, one with R and d chosen to best fit the data, the other with R and d ($d = \rho/\rho'$) evaluated at the $\frac{2}{10}$ density point of the ^{13}C charge density, calculated from an electron scattering parametrization.¹⁴ All nonanalog DCX transitions on $T=0$ target nuclei have the transition to the ground state being the strongest transition in the spectrum at forward angles. In the case of $^{13}\text{C}(\pi^+, \pi^-)^{13}\text{O}$, the transition to the 4.21 MeV state dominates at forward angles—in angular and energy (but not mass) dependence it fits in with nonanalog DCX on self-conjugate target nuclei.

In conclusion, the $^{13}\text{C}(\pi^+, \pi^-)^{13}\text{O}(\text{g.s.})$ angular distributions vary slowly between 0° and 50° . The excitation function distinguishes itself from other nonanalog DCX (ground state) to (ground state) transitions in that the excitation function is not peaked near 160 MeV.

The transition to the $E_x = 4.21 \text{ MeV}$ state exhibits features common to $\Delta J = 0$ nonanalog DCX reactions. The excitation function is peaked near 160 MeV and the angular distribution at 164 MeV has a simple diffractive shape, with a minimum consistent with the strong absorption radius. The similarities of the $^{12}\text{C}(\pi^+, \pi^-)^{12}\text{O}(\text{g.s.})$, $^{13}\text{C}(\pi^+, \pi^-)^{13}\text{O}(4.21 \text{ MeV})$, and $^{14}\text{C}(\pi^+, \pi^-)^{14}\text{O}(5.9 \text{ MeV})$ reactions cause us to speculate that the $^{13}\text{O}(4.21 \text{ MeV})$ state has $J^\pi = \frac{1}{2}^-$, thus allowing the reaction to proceed via a $\Delta J = 0$ process. Shell model calculations¹⁵ using a Cohen-Kurath p -shell effective interaction¹⁶ predict the existence of a $\frac{1}{2}^-$ state at $E_x = 4.0 \text{ MeV}$. Calculations of two-body isotensor matrix elements between these initial and final states are underway, and may shed light on the reaction mechanism of nonanalog double-charge exchange.

This work has been supported in part by The Natural Sciences and Engineering Research Council of Canada, The Robert A. Welch Foundation, The National Science Foundation, and The U.S. Department of Energy.

*Present address: Los Alamos National Laboratory, Los Alamos, NM 87545.

†Present address: Indiana University, Bloomington, IN 47401.

‡Permanent address: University of Pennsylvania, Philadelphia, PA 19104.

¹L. C. Bland, R. Gilman, M. Carchidi, K. Dhuga, C. L. Morris, H. T. Fortune, S. J. Greene, P. A. Seidl, and C. Fred Moore, Phys. Lett. **128B**, 157 (1983).

²P. A. Seidl, R. R. Kiziah, M. K. Brown, C. Fred Moore, C. L. Morris, H. Baer, S. J. Greene, G. R. Burselson, W. B. Cottingham, L. C. Bland, R. Gilman, and H. T. Fortune, Phys. Rev. C **30**, 973 (1984) (this issue).

³S. J. Greene, W. J. Braithwaite, D. B. Holtkamp, W. B. Cottingham, C. F. Moore, G. R. Burselson, G. S. Blanpied, A. J. Viescas, G. H. Daw, C. L. Morris, and H. A. Thiessen, Phys. Rev. C **25**, 927 (1982); M. O. Kaletka, Ph.D. thesis, Northwestern University, 1983; Los Alamos National Laboratory Report No. LA-9947-T, 1984 (unpublished).

⁴S. J. Greene, C. J. Harvey, P. A. Seidl, R. Gilman, E. R. Siciliano, and M. B. Johnson (unpublished).

⁵L. C. Liu, Phys. Rev. C **27**, 1611 (1983).

⁶S. J. Greene, D. B. Holtkamp, W. B. Cottingham, C. F. Moore, G. R. Burselson, C. L. Morris, H. A. Thiessen, and H. T. Fortune, Phys. Rev. C **25**, 924 (1982); R. Gilman, L. C. Bland, Peter A. Seidl, C. Fred Moore, C. L. Morris, Steven J. Greene, and H. T. Fortune, Nucl. Phys. (to be published).

⁷H. A. Thiessen, J. C. Kallne, J. F. Amann, R. J. Peterson, S. J. Greene, S. L. Verbeck, G. R. Burselson, S. G. Iverson, A. W. Obst, K. K. Seth, C. F. Moore, J. E. Bolger, W. J. Braithwaite, D. C. Slater, and C. L. Morris, Los Alamos Scientific Laboratory Report No. LA-6663-MS, 1977.

⁸S. J. Greene, W. J. Braithwaite, D. B. Holtkamp, W. B. Cottingham, C. F. Moore, C. L. Morris, H. A. Thiessen, G. R. Burselson, and G. S. Blanpied, Phys. Lett. **88B**, 62 (1979); S. J. Greene, Ph.D. thesis, The University of Texas at Austin, Los Alamos National Laboratory Report No. LA-8891-T, 1981.

- ⁹J. R. Carter, D. V. Bugg, and A. A. Carter, *Nucl. Phys. B* **58**, 378 (1973).
- ¹⁰P. Couvert, G. Bruge, R. Beurtey, A. Boudard, A. Chaumeaux, M. Garcon, D. Garreta, P. C. Gugelot, G. A. Moss, S. Platchkov, J. P. Tabet, Y. Terrien, J. Thirion, L. Bimbot, Y. Le Bornec, and B. Tatischeff, *Phys. Rev. Lett.* **41**, 530 (1978).
- ¹¹G. R. Burleson, G. S. Blanpied, G. H. Daw, A. J. Viescas, C. L. Morris, H. A. Theissen, S. J. Greene, W. J. Braithwaite, W. B. Cottingham, D. B. Holtkamp, I. B. Moore, and C. F. Moore, *Phys. Rev. C* **22**, 1180 (1980).
- ¹²K. K. Seth, in *Intermediate-Energy Nuclear Chemistry Workshop*, Los Alamos National Laboratory Report No. LA-8835-C, 1980.
- ¹³R. D. Amado, J.-P. Dedonder, and F. Lenz, *Phys. Rev. C* **21**, 647 (1980).
- ¹⁴C. W. de Jager, H. de Vries, and C. de Vries, *At. Data Nucl. Data Tables* **14**, 479 (1974).
- ¹⁵W. D. M. Rae, A. Etchegoyen, N. S. Godwin, and B. A. Brown, OXBASH, The Oxford-Buenos Aires Shell Model Code, 1983 (unpublished).
- ¹⁶S. Cohen, and D. Kurath, *Nucl. Phys.* **73**, 1 (1965).